

## High-temperature series expansions for the (2+1)-dimensional Ising model

This article has been downloaded from IOPscience. Please scroll down to see the full text article.

1990 J. Phys. A: Math. Gen. 23 1775

(<http://iopscience.iop.org/0305-4470/23/10/018>)

View [the table of contents for this issue](#), or go to the [journal homepage](#) for more

Download details:

IP Address: 129.252.86.83

The article was downloaded on 01/06/2010 at 08:34

Please note that [terms and conditions apply](#).

# High-temperature series expansions for the $(2+1)$ -dimensional Ising model

H-X He, C J Hamer and J Oitmaa

School of Physics, University of New South Wales, PO Box 1, Kensington 2033, NSW, Australia

Received 11 December 1989

**Abstract.** Using efficient cluster expansion methods, the known high-temperature series for the vacuum energy, specific heat, susceptibility and mass gap of the  $(2+1)$ -dimensional Ising model on the square and triangular lattices have been extended by several terms. Estimates of the critical indices demonstrate very convincing universality with the Euclidean version of the model.

## 1. Introduction

The three-dimensional Ising model provides a paradigm of all phase transitions. Its equivalent in lattice Hamiltonian field theory is the  $(2+1)$ -dimensional Ising model, and the principle of universality tells us that the critical behaviour of these two models should be the same. Now universality has been shown to hold exactly for various models in two dimensions, but in three dimensions this is not the case, and it is important to check as accurately as possible that the principle holds good. With this purpose in mind, we have set out to calculate some further terms in the high-temperature series expansions for the  $(2+1)$ -dimensional model.

Cluster expansion methods have been used previously by Hamer and Irving (1984b) and Hamer and Guttman (1989) to calculate high-temperature series for this model, but these earlier works did not use the most efficient algorithm possible to generate the required cluster configurations. By correcting this defect, we have been able to make very substantial extensions of these series. Low-temperature expansions for the model have previously been calculated by Pfeuty and Elliott (1971) and Marland (1981).

In section 2 of the paper the cluster expansion methods of Nickel (1980) are reviewed, together with our techniques for generating clusters and their associated series. In section 3 the resulting series are presented and analysed, and our conclusions are discussed in section 4. The accuracy of the exponent estimates does not improve as much as we might have hoped; but still the consistency with the Euclidean model results is very satisfactory.

## 2. Cluster expansion method

The cluster expansion methods which we use were first proposed by Nickel (1980), and were described in later papers by Marland (1981), Irving and Hamer (1984) and

Hamer and Irving (1984b). For convenience, let us briefly paraphrase the basic arguments due to Nickel.

Consider a lattice Hamiltonian of the form

$$H = H_0 + xV \quad (2.1)$$

where  $H_0$  is diagonal in the chosen set of basis states, and  $V$  is to be treated as a perturbation. For instance, in the present case the (2+1)-dimensional Ising model Hamiltonian is

$$H = \sum_i (1 - \sigma_3(i)) - x \sum_{\langle ij \rangle} \sigma_1(i)\sigma_1(j) - h \sum_i \sigma_1(i) \quad (2.2)$$

where  $\langle ij \rangle$  denotes nearest-neighbour pairs of sites on the two-dimensional spatial lattice, the  $\sigma_k$  are Pauli matrices acting on a two-state spin variable at each site,  $x$  corresponds to the inverse temperature  $\beta$  in the Euclidean formulation, and  $h$  is the magnetic field variable. Setting  $h = 0$  for the moment, we choose a representation where  $\sigma_3(i)$  is diagonal, and take

$$H_0 = \sum_i (1 - \sigma_3(i)) \quad (2.3)$$

$$V = - \sum_{\langle ij \rangle} \sigma_1(i)\sigma_1(j) \quad (2.4)$$

so that each term in  $V$  'flips' the spins on a nearest-neighbour pair of sites  $\langle ij \rangle$ .

From the eigenvalue equation for the system, one can derive by standard methods an iterative perturbation expansion for the energy  $E_n$  of the  $n$ th eigenstate:

$$E_n = E_n^0 + x \langle n | V | n \rangle + \sum_{k=2}^{\infty} x^k \left\langle n \left| V \left( \frac{P}{E_n - H_0} V \right)^k \right| n \right\rangle \quad (2.5)$$

where  $|n\rangle$ ,  $E_n^0$  are the unperturbed eigenvector and eigenvalue, and  $P$  is a projection operator onto all states *except*  $|n\rangle$ . Substituting iteratively for  $E_n$  on the right-hand side, one arrives at the less elegant but more explicit Rayleigh-Schrödinger expansion

$$E_n = E_n^0 + x \langle n | V | n \rangle + x^2 \left\langle n \left| V \frac{P}{E_n^0 - H_0} V \right| n \right\rangle + \dots \quad (2.6)$$

Now let us consider two states of our system more closely, namely the ground state and the first excited state. For simplicity, we assume periodic boundary conditions.

### 2.1. Ground-state energy

The ground state is invariant under spatial transformations: in the Ising model at  $x = 0$  it corresponds to the state  $|0\rangle$  with  $\sigma_3(i) = +1$  on every site. One can always normalise the energy such that  $E_0^0 = 0$ . Then each term in the series (2.5) or (2.6) involves various powers of the operator  $V$ . The series can now be rearranged according to site labels, grouping together all terms which involve perturbations (in this case, flip operators  $\sigma_1$ ) acting on each particular subset of sites on the lattice. Now the contribution of each such 'cluster' of sites is independent of its position on the lattice, and depends only on its topology or connectedness structure: so the terms can then be grouped into topologically distinct classes, and the ground-state energy on a large lattice of  $N$  sites can be written

$$E_0^N = \sum_{\alpha} C_{\alpha}^N \epsilon_{\alpha} \quad (2.7)$$

where  $C_\alpha^N$  is the number of ways of embedding a cluster of topology  $\alpha$  on the lattice of  $N$  sites, and  $\epsilon_\alpha$  is the contribution of one such cluster. In the case at hand, the sites are connected via the 'link' operators  $\sigma_1(i)\sigma_1(j)$ , and the constants we need are the so-called 'weak embedding constants' (Domb 1974).

One can similarly write the ground-state energy on any finite cluster of sites  $\beta$  as

$$E_0^\beta = \sum_\alpha C_\alpha^\beta \epsilon_\alpha \tag{2.8}$$

where  $C_\alpha^\beta$  is the number of ways of embedding cluster  $\alpha$  into cluster  $\beta$ . Now if the sites in the cluster  $\beta$  are not all connected, so that  $\beta$  can be split into two disconnected parts  $\beta_1$  and  $\beta_2$ , then  $E_0^\beta$  can be written as a simple sum:

$$E_0^\beta = E_0^{\beta_1} + E_0^{\beta_2}. \tag{2.9}$$

Writing this out in terms of the  $\epsilon_\alpha$ , one immediately sees that  $\epsilon_\beta$  must be identically zero, because one cannot embed cluster  $\beta$  into its sub-clusters  $\beta_1$  and  $\beta_2$ : so only connected or linked clusters contribute to  $E_0$  in the end, as we would expect. In a diagrammatic approach  $\epsilon_\alpha$  is made up of all the perturbation theory diagrams which span the entire cluster  $\alpha$  (Hamer and Irving 1984a).

Equation (2.8) provides an avenue for efficient calculation of the  $\epsilon_\alpha$ . One can calculate  $E_0^\beta$  by standard methods (see below), and then the corresponding 'cumulant' energy  $\epsilon_\beta$  can be found by inverting (2.8):

$$\epsilon_\beta = E_0^\beta - \sum_{\alpha'} C_{\alpha'}^\beta \epsilon_{\alpha'} \tag{2.10}$$

where the index  $\alpha'$  now runs over all the *smaller* sub-clusters embedded in  $\beta$ . So by starting with the smallest linked clusters and working upwards, one may generate a list of the  $\epsilon_\beta$  up to some maximum cluster size. These may then be inserted into equation (2.7) to give the bulk energy  $E_0^N$ .

If the energies  $E_0^\beta$  and  $\epsilon_\beta$  are expressed as power series in  $x$ , then the first non-zero term in  $\epsilon_\beta$  is  $O(x^m)$ ,  $m \geq n$ , where  $n$  is the number of links in the cluster, because it takes at least one power of  $V$  to span each link in the cluster. Thus we obtain a series for  $E_0^N$  which is exact up to a maximum order corresponding to the maximum cluster size.

### 2.2. First excited-state energy

Here we shall restrict ourselves specifically to the (2+1)-dimensional Ising model, although the method may be applied more generally. The unperturbed eigenvector corresponding to the first excited state is

$$|1\rangle = \sum_{i=1}^N \sigma_1(i) |0\rangle \tag{2.11}$$

where  $|0\rangle$  is the unperturbed ground state. Thus  $|1\rangle$  is a spatially invariant combination of all states with a single spin 'flip'. Note the normalisation  $\langle 1|1\rangle = N$ .

A perturbation expression for the energy of this state after two iterations may then be written as

$$E_1 = E_1^0 + \frac{x}{N} \langle 1|V|1\rangle + \frac{x^2}{N} \left\langle 1 \left| V \frac{P}{E_1 - H} V \right| 1 \right\rangle. \tag{2.12}$$

Next, Nickel argues that since the mass gap

$$F = E_1 - E_0 \quad (2.13)$$

is  $O(N^0)$  while  $E_0$  is  $O(N^1)$ , we may replace  $E_1$  by  $F$  in the denominator  $E_1 - H$ , throw away all terms of higher order in  $N$ , and write

$$F = E_1^0 + \frac{x}{N} \langle 1 | V | 1 \rangle + x^2 \frac{\Delta}{N} \quad (2.14)$$

where

$$\Delta = \left\langle 1 \left| V \frac{P}{F-H} V \right| 1 \right\rangle \Big|_{O(N^1)} \quad (2.15)$$

i.e.  $\Delta$  incorporates only those terms of order one in  $N$ . Since  $E_0^0 = 0$  and  $E_0$  is  $O(x^2 N)$ , the subtraction of  $E_0$  from  $E_1 - H$  in the denominator affects only terms of higher order in  $N$  in the perturbation expansion, and therefore has no effect on (2.15).

An iterative perturbation expansion for the quantity  $\Delta$  can be written down in the usual manner, expanding in powers of  $V$ :

$$\Delta = \left\langle 1 \left| V \frac{P}{F-H_0} V \right| 1 \right\rangle + \left\langle 1 \left| V \frac{P}{F-H_0} V \frac{P}{F-H_0} V \right| 1 \right\rangle + \dots \Big|_{O(N^1)}. \quad (2.16)$$

We can now go through an argument much the same as for the ground-state energy, to show that on the  $N$ -site lattice

$$\Delta^N = \sum_{\alpha} C_{\alpha}^{N'} \delta_{\beta'} \quad (2.17)$$

while on a finite cluster of sites  $\beta'$

$$\Delta^{\beta'} = \sum_{\alpha'} C_{\alpha'}^{\beta'} \delta_{\beta}. \quad (2.18)$$

so that the quantities  $\delta_{\beta'}$  can be calculated by working up from small clusters to large ones just as for the ground-state energy. The major difference is that the mass gap does not obey the addition law (2.9), and so we cannot restrict ourselves only to *linked* clusters. The index  $\alpha'$  runs over both connected and disconnected clusters; and the  $C_{\alpha}^{N'}$  are the terms of order  $N$  in the embedding constant of cluster  $\alpha'$  in the  $N$ -site lattice.

### 2.3. Clusters and embedding constants

To proceed with the derivation of series by this method it is necessary to obtain the following data:

(a) a list of all clusters which give contributions to the series, up to the order required;

(b) the embedding constants  $C_{\alpha}^{N'}$  of the clusters for the lattice under consideration, in our case the square and triangular lattices;

(c) for each cluster  $\alpha$ , a list of sub-clusters  $\beta$  and corresponding embedding constants  $C_{\alpha}^{\beta}$ .

We have developed an efficient algorithm† for generating the list of clusters. Each cluster corresponds to a connected graph (see Domb (1974) for graph theoretical

† This is based on a program and unpublished work of C J Elliott.

concepts pertinent to this work). All graphs of  $n_v$  vertices and  $n_b$  bonds can be generated by starting with  $n_v$  isolated vertices and adding  $n_b$  lines joining pairs of vertices, in all possible ways. As is well known, the number of graphs increases exponentially with size and it is inefficient to generate graphs which do not, in fact, contribute to the final series. Therefore various constraints are imposed: for example, on the square lattice no graph with a vertex of order 5 or more and no graph which contains a triangle can contribute, so such graphs are eliminated during the generation process.

For the susceptibility, which involves two 'magnetic' operators and any number of 'thermal' operators, the lowest order at which a graph contributes is given by the following rule.

Consider the bare graph and all graphs obtained from it by replacing one or more single bonds by double bonds. The order is the least number of bonds yielding a graph with either 0 or 2 vertices of odd order. This is illustrated in figure 1(a).

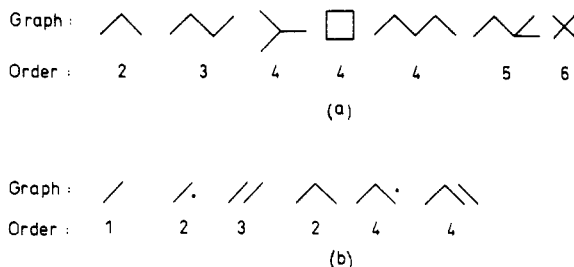


**Figure 1.** (a) Examples of clusters which contribute to the susceptibility, together with the lowest order in  $x$  at which they enter. (b) Examples of clusters which contribute to the mass gap, together with the lowest order in  $x$  at which they enter.

After the graph list has been produced the embedding constants or 'lattice constants' are obtained via direct enumeration using a fairly standard computer program. Another program is used to find subgraphs for any given graph, by testing whether each of the preceding graphs in the list can be embedded in it. At the same time the embedding constant is obtained.

In this way we have generated the data required to compute the ground-state energy and susceptibility through order 16 for the square lattice and order 14 for the triangular lattice. The number of graphs which contribute in each case are:

square lattice (order 16)	13 271 graphs
triangular lattice (order 14)	33 522 graphs.

For the mass gap series the procedure is similar, in general terms. However in this case disconnected graphs, including graphs with a single isolated vertex, also contribute. These are simply generated from the connected graph list, and the lattice constants are obtained by an algebraic procedure which is also computerised. In this case the rule for the minimum order is as follows.

Consider the bare graph and all double-bond derivatives as before. Then:

- (i) if the graph has no isolated vertex, the number of odd vertices must be 0 or 2;
- (ii) if the graph has an isolated vertex, the number of odd vertices must be 0.

This is illustrated in figure 1(b).

We have generated the data required for the mass gap series through order 13 for the square lattice and through order 12 for the triangular lattice. The number of graphs (without isolated vertices) which contribute are:

square lattice (order 13)	2223 graphs
triangular lattice (order 12)	6831 graphs.

#### 2.4. Cluster energies

The second major element of the program is the calculation of the cluster energies  $E_0^\beta$ , or  $\Delta^\beta$  for the mass gap. The first step is to generate the Hamiltonian matrix for a given cluster. The basis states can be conveniently labelled by their binary spin code (0 or 1 for each site depending whether the spin  $\sigma_3$  is +1 or -1): there are  $2^{n_v}$  states for a cluster of  $n_v$  vertices. Then the Hamiltonian matrix can be given as three separate lists.

(i)  $H_0$  is diagonal, and contains  $2^n$  elements, which may be obtained simply by counting the number of 'down' spins in each basis state.

(ii) The 'thermal' perturbation operator  $V$  contains  $n_b$  'link' operators  $\sigma_1(i)\sigma_1(j)$  for a cluster of  $n_b$  bonds, and thus contains  $2^{n_b} \times n_b$  non-zero elements. The matrix element is unity in each case, so we list only the final states corresponding to each given initial state.

(iii) The 'magnetic' perturbation operator contains  $n_v$  'site' operators  $\sigma_1(i)$ , and so contains  $2^{n_v} \times n_v$  non-zero elements, which are listed in a similar fashion.

Once the Hamiltonian matrix elements are known, the corresponding energy  $E_0^\beta$  can be calculated as a power series by an efficient algorithm due to Hornby and Barber (1985). The perturbation expansion for  $\Delta^\beta$  has a similar structure, and can be calculated by a similar algorithm; except that in this latter case, the mass gap  $F$  itself appears in the energy denominators in equation (2.16). Hence one must proceed in an iterative manner: having computed  $F$  to  $O(x^n)$ , one must feed it back into the energy denominators and begin the computations all over again from scratch to get it correct to  $O(x^{n+1})$ . This is not necessary for the ground-state energy.

Having obtained the  $E_0^\beta$ , it is a simple matter of combinatorics to obtain the cumulant energies  $\varepsilon_\beta$ , and the final bulk energy  $E_0^N$ . The entire set of calculations occupied some 220 CPU hours on an IBM 3090, using quadruple precision.

### 3. Results and analysis

From the ground-state energy one can derive series for the 'specific heat'

$$\tilde{C}(x) = -\frac{x^2}{N} \frac{\partial^2 E_0}{\partial x^2} \quad (3.1)$$

$$\underset{x \rightarrow x_c}{\sim} (x_c - x)^{-\alpha} \quad (3.2)$$

(where  $x_c$  is the critical point) and the susceptibility

$$\chi(x) = -\frac{1}{N} \frac{\partial^2 E_0}{\partial h^2} \Big|_{h=0} \quad (3.3)$$

$$\underset{x \rightarrow x_c}{\sim} (x_c - x)^{-\gamma}. \quad (3.4)$$

The mass gap behaves as

$$F \underset{x \rightarrow x_c}{\sim} (x_c - x)^\nu. \tag{3.5}$$

Table 1 lists coefficients of the perturbation series in  $x$  for the ground-state energy per site,  $E_0/N$ , the susceptibility  $\chi$  and the mass gap  $F$ . The coefficients up to ninth order on the square lattice and eighth order on the triangular lattice were previously calculated by Hamer and Guttman (1989).

3.1. Padé approximants

From the series for the susceptibility, the mass gap and the specific heat, we have extracted estimates for the critical point and the critical index using standard Padé methods (Guttman 1989). Unbiased estimates are obtained from Padé approximants

**Table 1.** High-temperature series in  $x$  for the vacuum energy per site  $E_0/N$ , the susceptibility  $\chi$  and the mass gap  $F$ . Coefficients of  $x^n$  are listed for the square lattice (upper half) and triangular lattice (lower half).

$n$	$E_0/N$	$\chi$	$F$
0	0	1	2
1	0	4	-4
2	-0.5	13.5	-2
3	0	45	-3
4	-0.46875	144.84375	-4.5
5	0	464.444444444	-11
6	-1.1484375	1469.35850694	-20.5078125
7	0	4639.48234954	-57.69921875
8	-4.395263671875	14544.1192397	-114.836303711
9	0	45537.4796633	-350.106719971
10	-20.6786155701	141947.730164	-730.535977681
11	0	442100.534692	-2312.13459937
12	-110.752848078	1372818.04093	-5002.70683153
13	0	4260277.89708	-16167.3575508
14	-647.484427534	13192459.0985	
15	0	40832888.3912	
16	-4033.21806935	126179285.813	
0	0	1	2
1	0	6	-6
2	-0.75	32.95	-6
3	-0.75	166.5	-10.5
4	-1.359375	843.046875	-31.5
5	-3.09375	4218.41666667	-98.53125
6	-8.35546875	20941.0230035	-346.7109375
7	-24.66796875	103361.512587	-1255.20556641
8	-78.1272583008	507986.371687	-4795.43701172
9	-260.223449707	2488222.50870	-186577.8698883
10	-902.046897888	12155136.2137	-74627.2885151
11	-3227.54874810	59248156.0755	-302784.980111
12	-11852.6421807	288265613.837	-1248795.45214
13	-44479.5726107	1400348157.31	
14	-170007.969892	6793608696.09	



to the logarithmic derivative of the function; and once the critical point is known, a 'biased' estimate of the critical index can be obtained from Padé approximants to  $(x_c - x)(d/dx) \log F(x)|_{x=x_c}$ .

The best-behaved series, as one might expect, is the susceptibility on the triangular lattice. Unbiased estimates of the critical parameters obtained from the Dlog Padés are listed as an example in table 2. There is no objective way of finding the error in such estimates: as a rule of thumb, we have taken the spread between the last several entries in the Padé table and multiplied it by a factor of two or three. We note a consistent downward trend in the last few estimates of the index  $\gamma$ , which indicates the true value is somewhat below 1.244. (The final results for the various series are listed in table 4 below.)

For the specific heat series, the Padé approximant tables gave no stable or sensible result. This is a well known phenomenon, attributed to an additive, regular term in the specific heat at the critical point.

**Table 2.** Dlog Padé approximants to the susceptibility on the triangular lattice. An asterisk denotes a defective approximant.

<i>N</i>	[ <i>N</i> / <i>N</i> -1 ]		[ <i>N</i> / <i>N</i> ]		[ <i>N</i> / <i>N</i> +1 ]	
	Pole	Residue	Pole	Residue	Pole	Residue
2	0.209 61	(1.2432)	0.209 75	(1.2465)	0.209 76	(1.2468)
3	0.209 76	(1.2469)	0.209 74	(1.2464)*	0.209 70	(1.2478)
4	0.209 80	(1.2483)	0.209 78	(1.2475)	0.209 76	(1.2462)
5	0.209 78	(1.2472)	0.209 70	(1.2377)*	0.209 74	(1.2441)
6	0.209 74	(1.2449)	0.209 74	(1.2444)	0.209 74	(1.2442)
7	0.209 73	(1.2436)				

### 3.2. Ratio methods

Ratio methods for the estimation of critical parameters have also been discussed by Guttman (1989). If a function *F* has a series expansion

$$F(z) = \sum_{n=0}^{\infty} a_n z^n \tag{3.6}$$

and behaves like

$$F(z) \sim A \left( 1 - \frac{z}{z_c} \right)^{-\lambda} + B \tag{3.7}$$

as  $z \rightarrow z_c^-$ , then the ratios

$$r_n = \frac{a_n}{a_{n-1}} \underset{n \rightarrow \infty}{\sim} \frac{1}{z_c} \left( 1 + \frac{\lambda - 1}{n} \right) \tag{3.8}$$

and an even better estimate of the critical point can be obtained from the linear

extrapolants

$$1_n = nr_n - (n-1)r_{n-1} = \frac{1}{z_c} \left( 1 + O\left(\frac{1}{n^2}\right) \right). \tag{3.9}$$

Unbiased estimates of the critical index can be obtained from

$$\frac{n(2-n)r_n + (n-1)^2 r_{n-1}}{nr_n - (n-1)r_{n-1}} = \lambda + O\left(\frac{1}{n}\right) \tag{3.10}$$

while if the critical point is known, biased estimates of  $\lambda$  are given by

$$nz_c r_n - n + 1 = \lambda + O\left(\frac{1}{n}\right). \tag{3.11}$$

A graph of the linear extrapolants  $1_n$  against  $1/n$  is shown for the triangular lattice susceptibility in figure 2. After jumping around for a while, the sequence of  $1_n$  values settles down to a quite stable and consistent trend line. We have tried various methods for extrapolating this sequence to the limit  $n \rightarrow \infty$ , such as Brezinski's  $\theta$  algorithm, the Levin  $u$  transform, the Barber-Hamer algorithm, and the Neville-Aitken table, which have all been discussed by Guttman (1989). Unfortunately, the sequence is not smooth enough for these methods to work at all well<sup>†</sup>, and we have found no better technique than a simple extrapolation with ruler and pencil, as shown in figure 2. The stability of the result can be tested by 'end-shifting' the sequence,  $n \rightarrow n + \epsilon$  in equation (3.9). Hence we obtain a final result as listed in table 4 below.

Unbiased estimates of the critical index  $\gamma$  obtained from equation (3.10) are graphed against  $1/n$  in figure 3. The sequence shows similar behaviour to the  $1_n$  values.

For the square lattice, the ratio method estimates oscillate strongly between even and odd  $n$  values, due to the antiferromagnetic singularity present for this loose-packed

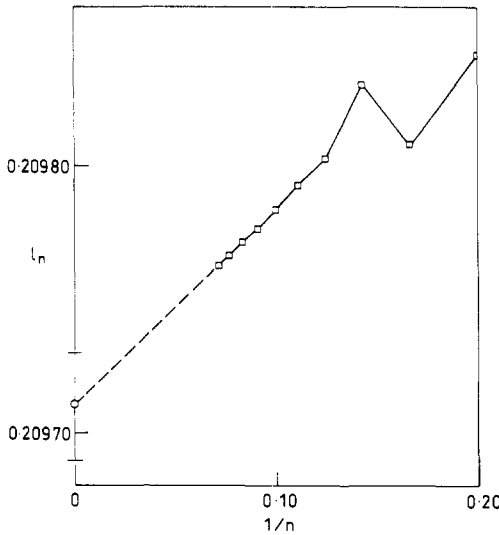


Figure 2. Linear extrapolants  $1_n$  for the triangular lattice susceptibility plotted against  $1/n$ . A straight line drawn to the axis gives our final estimate of the critical point.

<sup>†</sup> Guttman (1989) advocates the use of an Euler transformation to 'smooth' the sequence beforehand, but we found this technique was of little help.

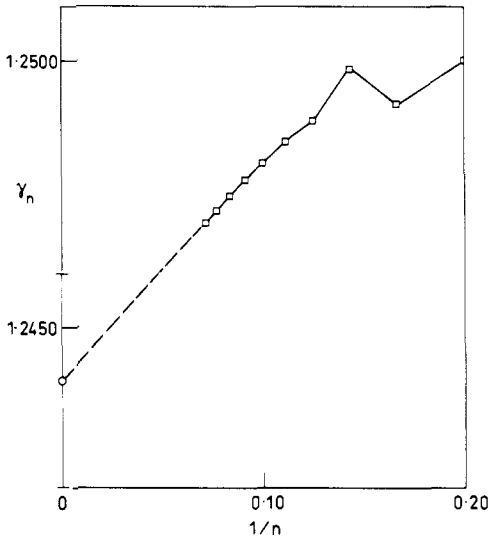


Figure 3. Unbiased estimates of the critical index  $\gamma$  obtained from the triangular lattice susceptibility ratios, plotted against  $1/n$ .

lattice. We have used standard techniques to minimise this, but the final results are inevitably less accurate. The mass gap ratios on both lattices are also very 'noisy', and no very good estimate of the index  $\nu$  was obtained by this method.

### 3.3. Differential approximants

Differential approximants (Guttman 1989) can be regarded as generalisations of Padé approximants, and have the advantage that they can accommodate more complicated singularity structures. The inhomogeneous differential approximants, for instance, can handle a function such as the specific heat which has an additive regular part: and indeed these approximants are found to be much more successful in estimating the specific heat index  $\alpha$ . For the mass gap, on the other hand, there is no additive regular part, and the homogeneous approximants perform much better than the inhomogeneous ones. In principle, the differential approximants should be able to handle confluent singularities as well, which are certainly expected to be present in this model; but the outcome for  $\gamma$  and  $\nu$  does not show any great difference between Padé and differential approximants; nor did we see any great difference between the first- and second-order differential approximants.

A table of differential approximants obtained using program NEWQGRD (Guttman 1989) for the triangular lattice susceptibility is presented as an example in table 3. Our critical parameter estimates obtained by all three methods are summarised in table 4.

## 4. Conclusions

Selecting the results which appear to be most accurate from table 4, we arrive at the final estimates listed in table 5. Also listed there are some of the best previous estimates

**Table 3.** Table of first-order differential approximants to the triangular lattice susceptibility. Estimates of  $x_c$  and  $\gamma$  (in brackets) are shown which come from the  $[L/N + \Lambda; N]$ ,  $\Lambda = -1, 0, 1$ , approximants, in the notation of Gittmann (1989). Defective approximants are asterisked.

	$\Lambda$	$N = 4$	$N = 5$	$N = 6$
$L = 1$	-1	0.209 64 (-1.233)	0.209 74 (-1.243)	0.209 74 (-1.243)
	0	0.209 75 (-1.245)	0.209 74 (-1.243)	0.209 73* (-1.243)
	+1	0.209 74 (-1.243)	0.209 74 (-1.243)	
$L = 2$	-1	0.209 68 (-1.237)	0.209 76* (-1.237)	0.209 73 (-1.241)
	0	0.209 73 (-1.243)	0.209 73 (-1.243)	
	+1	0.209 75* (-1.245)	0.209 73 (-1.241)	
$L = 3$	-1	0.209 74 (-1.244)	0.209 73 (-1.243)	
	0	0.209 74 (-1.243)	0.209 73 (-1.241)	
	+1	0.209 73 (-1.242)		
$L = 4$	-1	0.209 72 (-1.239)	0.209 73 (-1.242)	
	0	0.209 73 (-1.243)		
	+1	0.209 73 (-1.241)		

**Table 4.** Table of critical parameter estimates obtained by each of the various methods. Specific heat  $C \sim (x - x_c)^{-\alpha}$ ; magnetic susceptibility  $X \sim (x - x_c)^{-\gamma}$ ; mass gap  $F \sim (x - x_c)^\nu$ .

Method	Critical point $x_c$	Critical index					
		Unbiased			Biased		
		$\gamma$	$\nu$	$\alpha$	$\gamma$	$\nu$	$\alpha$
Triangular lattice							
Padés	0.209 74 (3)	1.244 (3)	0.641 (3)	—	1.241 (3)	0.636 (4)	—
Ratios	0.209 71 (2)	1.244 (2)	—	0.16 (3)	1.241 (3)	0.63 (1)	0.12 (2)
Diff. ( $K = 1$ )	0.209 73 (2)	1.242 (2)	0.640 (4)	0.12 (2)	1.240 (4)	0.636 (4)	0.10 (2)
Approx. ( $K = 2$ )	0.209 74 (4)	1.243 (5)	0.642 (8)	0.11 (8)	1.240 (4)	0.640 (4)	0.10 (2)
Square lattice							
Padés	0.328 50 (10)	1.245 (5)	0.641 (10)	—	1.245 (3)	0.638 (2)	—
Ratios	0.328 4 (3)	1.245 (3)	—	0.15 (5)	1.244 (3)	—	0.12 (2)
Diff. ( $K = 1$ )	0.328 51 (8)	1.244 (6)	0.642 (5)	—	1.244 (4)	0.637 (4)	0.11 (2)
Approx. ( $K = 2$ )	0.328 50 (4)	1.244 (4)	0.645 (10)	—	1.244 (4)	0.643 (8)	—

**Table 5.** A comparison of the results obtained in the present work with some previous calculations. HT = high-temperature series; LT = low-temperature series; FS = finite-size scaling; MC = Monte Carlo; (b) = biased; (ub) = unbiased.

	$\gamma$	$\nu$	$\alpha$	$x_c$
<b>(2+1)-dimensional Ising model</b>				
<b>Triangular lattice</b>				
LT Marland 1981	1.250 (12)	—	( $\alpha'$ )0.098 (3)	0.209 8 (2)
FS Hamer and Johnson 1986	1.236 (8)	0.627 (4)	—	0.209 8 (2)
HT Hamer and Guttman 1989 (ub)	1.243 (4)	0.646 (8)	—	
	(b) 1.242 (2)	0.640 (5)	—	0.209 72 (7)
This work (ub)	1.242 (2)	0.641 (3)	0.12 (2)	0.209 72 (2)
	(b) 1.241 (3)	0.636 (4)	0.10 (2)	
<b>Square lattice</b>				
LT Marland 1981	1.25	—	—	0.329 (1)
FS Henkel 1984	—	0.629 (2)	—	0.328 (1)
HT Hamer & Guttman (ub)	1.239 (5)	0.646 (8)	—	0.328 5 (4)
	(b) 1.245 (4)	0.640 (5)	—	
This work (ub)	1.245 (3)	0.642 (5)	0.15 (5)	0.328 50 (4)
	(b) 1.244 (3)	0.638 (2)	0.11 (2)	
<b>Three-dimensional Ising model</b>				
HT Guttman 1987	1.239 (3)	0.632 (3)		
MC Bhanot <i>et al</i> 1989		0.6295 (10)		
<b>Field theory estimate</b>				
LeGuillou and Zinn-Justin 1980	1.241 (2)	0.630 (2)	0.110 (5)	

by other authors. Allowing for a little optimism in the error bars here and there, the critical exponents for the two lattices agree very well. For the index  $\gamma$ , they also agree with estimates from the three-dimensional model and field theory. For the index  $\nu$ , our estimates are still a little high: this is a common problem with high-temperature series estimates, and we observe a definite tendency for the estimates to decrease as more terms of the series are included.

Our calculations have added four new terms to the mass-gap series for each lattice, and six and seven terms to the ground-state energy and susceptibility on the triangular and square lattices, respectively. We have substantially improved estimates for the critical points, but the improvement for the critical indices is rather slight. Nevertheless the results bear out once more the universality between these two Hamiltonian lattice field theories and their Euclidean analogues.

### Acknowledgments

We are very grateful to Professor Guttman for providing us with a copy of his program NEWQGRD, and for general advice and assistance regarding the series analysis. The work of H-XH was supported by an Australian Research Council Fellowship.

**References**

- Bhanot G, Salvador R, Black S, Carter P and Toral R 1987 *Phys. Rev. Lett.* **59** 803
- Domb C 1974 *Phase Transitions and Critical Phenomena* vol 3, ed C Domb and M S Green (New York: Academic)
- Guttman A J 1987 *J. Phys. A: Math. Gen.* **20** 1855
- 1989 *Phase Transitions and Critical Phenomena* vol 13, ed C Domb and J Lebowitz (New York: Academic)
- Hamer C J and Guttman A J 1989 *J. Phys. A: Math. Gen.* **22** 3653
- Hamer C J and Irving A C 1984a *Nucl. Phys. B* **230** 336
- 1984b *J. Phys. A: Math. Gen.* **17** 1649
- Hamer C J and Johnson C H J 1986 *J. Phys. A: Math. Gen.* **19** 423
- Henkel M 1984 *J. Phys. A: Math. Gen.* **17** L795
- Hornby P G and Barber M N 1985 *J. Phys. A: Math. Gen.* **18** 827
- Irving A C and Hamer C J 1984 *Nucl. Phys. B* **230** 361
- Le Guillou J C and Zinn-Justin J 1980 *Phys. Rev. B* **21** 3976
- Marland L G 1981 *J. Phys. A: Math. Gen.* **14** 2047
- Nickel B G 1980 unpublished
- Pfeuty P and Elliott R J 1971 *J. Phys. C: Solid State Phys.* **4** 2370